Manganese Dioxide Based Supercapacitor

Naida Cicelly Tania, Ng Wei Kang, Feng Yuanyuan
Anderson Junior College
Singapore

Abstract— **In the face of the world's energy scarcity, Supercapacitor is a promising candidate of energy storage device for uses in future technologies as it has a superior charge/discharge rate. Furthermore, supercapacitors have a virtually unlimited charge cycle, which allows it to be re-used continuously, hence making it an efficient yet cost-effective energy storage device.**

However, supercapacitor is not widely used mainly because they have a low energy density, which means it is unable to store plenty of energy (~10%-20% that of a normal battery). This limits supercapacitors from delivering power over extended periods of time, making them less than ideal as an energy storage device.

Our aim is to investigate the properties that contribute in making a supercapacitor with a higher energy density by maximizing its specific capacitance (ability of a material to store energy per mass). To achieve this, we focus on Manganese Dioxide (MnO_2) nanoparticles, which have superior energy storage ability. We vary several parameters (concentration, temperature and precursor) of the samples made. This gives samples with different specific surface area and different stabilizing cation for the same crystal structure which will then affect the specific capacitance of the material.

Keywords-component; MnO_2; supercapacitor; specific capacitance; specific surface area; stabilising cation

I. BACKGROUND AND PURPOSE

1.1 Importance of energy storage

Fossil fuel is the most common source of energy used in the world. However, usage of fossil fuel is both costly and environmentally damaging. This will not be sustainable in the long run. Hence there is a need to search for alternative source of energy.

Electrochemical energy conversion has attracted considerable attention recently. In electrochemical energy, charge-transportation changes from ionic transport in the electrolyte to electronic transport in the electrode at the electrical interface. This minimizes the pollution to the environment while simultaneously maximizes the efficiency of the energy conversion.

The electron-transfer reactions lead to many important applications of electrochemistry, which include energy storage/conversion devices such as batteries, fuel cells and supercapacitors.

1.2 Supercapacitor

Supercapacitor is a system for electrochemical energy storage device similar to batteries and fuel cells. It works based on the charge storage at the phase boundary of the electrode/electrolyte interface. Unlike capacitors, supercapacitors store charges based on electrochemical reaction rather than static charge. Supercapacitors also have a superior charge/discharge rate, allowing it to deliver more power than batteries while also charging up much faster. Furthermore, supercapacitors have a virtually unlimited charge cycle so it becomes a cost-effective storage since it can be re-used continuously.

Although supercapacitors have greater specific capacitance (ability to store energy) than capacitors, it is still inferior compared to other energy storage device such as batteries (~10%-20% that of a normal battery). Because of this, usually while the battery supplies energy during normal power requirements, the capacitor supplements energy when high power requirements arise during starting, acceleration, change of gear, hill climbing, etc., for short durations. Supercapacitors are more reliable and faster working backup power sources than batteries. Small, low voltage capacitors are used for this purpose in a variety of products such as CD players, cameras, computers, telephones or electronic toys.

Supercapacitor is classified into two main types: Electrochemical Double Layer (EDL) and Redox supercapacitors. EDL supercapacitor consists of two layers. It operates based on the rearrangement of charges at the double layer of electrolyte near the electrode. The performance of such supercapacitors improve with greater surface area materials. Meanwhile, Redox supercapacitors operate based on the charge transfer reactions at the electrode/electrolyte interface. The electrons produced are transferred across the interface. The third type is a hybrid supercapacitors, which combines both EDL and redox supercapacitors.

1.3 Use of metal oxide

Transition metal oxides have attracted much attention as a electrode material for supercapacitors because of the following merits: variable oxidation state, excellent chemical and electrochemical stability, ease of preparation and handling. For supercapacitor, the use of metal oxide allows greater specific capacitance. Several transition metal oxides have come into spotlight: Iron, Manganese, Nickel, Cobalt, and Rubidium. RuO_2 prepared by sol-gel process at low temperature has a specific capacitance as high as 720 F g^{-1} compared to commercial supercapacitor that is working at maximum 25-30 F g^{-1} . However, high cost, low porosity and toxic nature of RuO_2 limit commercialization of supercapacitors using this material (Table 1). Hence, there is a need to investigate alternate transition metal oxides, which are cheap, non toxic, environmental friendly and available in abundance

Parameters	Fe	Mn	Ni	Co	Ru
Market price (\$ kg^{-1})	0.23	0.5	13	25	75
Atomic content in air (ppm)	50000	950	75	25	0.004
Permissible amount in air (mg m^{-3})	10	5	1	0.1	< 0.001
Permissible amount in water (mg m^{-3})	300	200	13.4	0.7	< 0.001

Table 1: Table showing the different transition metal oxides and its price and poison level

1.3.1 Manganese dioxide

Manganese dioxide (MnO_2) nanoparticles are commonly sought due to its advantages of being low cost, abundance in earth, environmental friendliness, and superior performance in energy capacity as compared to the other metal oxides mentioned before. It is the eleventh most abundant element in the world. MnO_2 acts like pseudo-capacitive materials material i.e it displays similar traits to capacitors such as the ability to store and discharge energy. However, MnO_2 is not used on its own because it has low conductivity.

Thus our project aims to investigate the ideal condition for MnO_2 nanoparticles in order to maximize the energy density of hybrid (metal oxide) supercapacitors.

II. HYPOTHESIS

Energy density is given by this equation:

$$E = \frac{1}{2} C . V$$

In order to improve the energy density (E) of the supercapacitor, the specific capacitance (C) or the cell voltage (V) has to be maximized. Specific capacitance is the ability of a specific mass of body to store electrical charges. We predict that by increasing the specific surface area of MnO_2 nanoparticles of the same crystal structure, we will be able to obtain the highest capacitance as there will be more active sites on the material to store energy. We will vary the concentration (0.01 M and 0.05 M) and the temperature (140°C and 400°C) used in synthetizing the samples to produce samples of different surface area. We hypothesized that increase in concentration will decrease the specific surface area as it will cause the MnO_2 nanoparticles to be bulkier. We also hypothesized that increase in temperature will decrease the specific surface area of the nanoparticles as it will cause the nanoparticles to clump together.

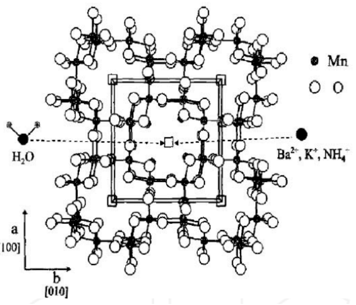

We will be using α -MnO_2 as the active material. α -MnO_2 consists of small (1x1) and larger (2x2) tunnels with cations (such as Ba^{2+} (hollandite), and K^+ (cryptomelane) and NH_4^+ and H_2O (or H_3O^+)) stabilizing the (2x2) tunnel in α -MnO_2 framework as shown in

Figure 2: The crystal structure of α -MnO_2

Studies have shown that larger tunnel size enhances ion diffusion (e.g. proton conductivity). Specific capacitance of MnO_2 is found to depend strongly on the crystallographic structure, and it decreases as the size of the tunnel decreases in the following order: $\alpha > \delta > \gamma > \lambda > \beta$. A specific capacitance value of 240 F g^{-1} is obtained for α-MnO_2, whereas it is 9 F g^{-1} for β-MnO_2. A wide (~ 4.6 Å) tunnel size and large surface area of α-MnO_2 are ascribed as favourable factors for its high specific capacitance. This means that it would be able to improve the reaction within the material for charge storage. We postulate that by altering the cation that stabilizes the MnO_2 nanoparticles by substituting it with different stabilizing cations (using K^+ and H_3O^+ as the cations), we will be able to obtain greater specific capacitance by changing the size of the tunnel. We will vary the precursor ($KMnO_4$ to $(H_3O)MnO_4$) used in synthetizing the MnO_2 nanoparticles.

Method and Materials

We prepared six different samples, each one consisting of three batches to test our hypotheses.

1) Control group consisting of only Nickel foam
2) Nickel foam with only carbon black
3) Nickel foam with carbon black and manganese oxide created using 0.01 mol dm^{-3} $KMnO_4$ precursor produced at 140^{0}c (sample 0.01M $KMnO_4$)
4) Nickel foam with carbon black and manganese oxide created using 0.05 mol dm^{-3} $KMnO_4$ precursor produced at 140^{0}c (sample 0.05M $KMnO_4$)
5) Nickel foam with carbon black and manganese oxide created using 0.05 mol dm^{-3} $KMnO_4$ precursor produced at 400^{0}c (sample alpha-K)
6) Nickel foam with carbon black and manganese oxide created using 0.05 mol dm^{-3} (H3O)MnO_4 precursor produced at 400^{0}c (sample alpha K-free)

Carbon black is used to increase MnO_2‘s conductivity.

Sample 1) and 2) act as controls is to calculate the specific capacitance of the non-active materials so that the results we obtain at the end is the true capacitance of our active material.

To synthesize sample 3), we use the following Cetyl trimethylammonium bromide (CTAB) as the surfactant to minimize clumping of the MnO_2 (0.05M, 10ml). Water in order to obtain a homogenous solution and as a solvent (10ml). And $KMnO_4$ as the precursor (0.01M, 2ml). The chemicals are heated in a round-bottomed flask (Figure3A). Oxidation of $KMnO_4$ will take place, giving us a brown solution of MnO_2 (aq) as our final product.

Next, the solutions are placed into a centrifuge (Figure 3B). This is to help separate the excess CTAB from the MnO_2 since CTAB will block the active sites of the MnO_2, thus impairing the performance of the sample. After each centrifuge, 10ml of water will be added to dissolve the MnO_2. It will be sonicated to ensure it is homogenous. Then 15ml of water will be added followed by 10ml acetone to separate the CTAB and the MnO_2. Three centrifuges are done in total to ensure complete removal of CTAB. The samples are dried afterwards to give a powder form of MnO_2

Sample 4) is made using samples of 0.05M of $KMnO_4$. Procedures are identical to those used for preparation of the 0.01M samples. We predict that higher concentrations of $KMnO_4$ will form bulkier MnO_2 nanoparticles.

Sample 5) is made of MnO_2 nanoparticles formed with higher temperature at 400°c. Due to safety concerns as preparation of samples involves the use of a blast furnace at 400°c, preparation of the sample is done by our external mentor. MnO_2 was synthesized by redox reaction between stoichiometric quantities of $MnSO_4$ and $KMnO_4$ in aqueous medium. In a typical synthesis in an aqueous medium, 20 mL of 0.05 M $KMnO_4$ solution was mixed with 10 mL of 0.15 M $MnSO_4.H_2O$ solution and stirred continuously for 6h. A dark-brown precipitate thus formed and was washed several times with distilled water, centrifuged, and dried at 70 °C in air for 12 h. Then the as-obtained powder was annealed at 400°C for 4h. We predict that the intense heat applied onto the powder will cause the MnO_2 nanoparticles to aggregate, resulting in a lower specific area than those formed in the previous two batches. We can use this to further test the effects of specific area on energy density.

Sample 6) is prepared using a different precursor ($(H_3O)MnO_4$) Due to safety concerns since high temperature was used, the preparation is also done by our external mentor. Powdered commercial Mn_2O_3 was heated at 700°C to remove impurities. The resulting material was then added to a 4 M H_2SO_4 solution to form an aqueous suspension. After heating at 80°C for 6 hours under stirring, the resulting product was centrifuged, decanted and washed with deionized H_2O and dried at 90°C in air to form nanocrystalline α-MnO_2. This will produce MnO_2 nanoparticles with H_3O^+ as the stabilizing cation.

To prepare the testing of the characteristics of all the samples, 8mg of the sample is mixed with 1mg of carbon black. The carbon black helps to increase the conductivity of the material tested. After mixing it into a homogenous mix, 19µm of NMP is added as binder. The chemicals are mixed together to form a slurry (Figure 3C). The slurry is applied onto a piece of nickel foam and is compressed under a gravity machine to ensure that the samples are adhesive to the substrate, ensuring better conductivity (Figure 3D).

We tested our samples using an electroanalytical technique known as cyclic voltammetry. We can then use the results to determine the specific capacitance of the material. Three types of electrodes are used:

A working electrode consisting of the sample, a counter electrode consisting of platinum sheet, and a reference electrode of saturated calomel electrode. The electrolyte used is 1M of Na_2SO_4. The voltage window is from 0 to 0.9V. Scanning rate of $2mVs^{-1}$, $5\ mVs^{-1}$, $10\ mVs^{-1}$, $20\ mVs^{-1}$, $50\ mVs^{-1}$, $100\ mVs^{-1}$, $200\ mVs^{-1}$, and $500\ mVs^{-1}$ are used. Graphs of current against the potential are obtained from the cyclic voltammogram (CV) function

III. RESULT AND DISCUSSION

Specific capacitance is given by this equation:

$$C = \frac{\int I.\Delta V}{2V.m.u}$$

Where $\int I.\ \Delta V$= area of CV curve, V= potential window (0.9V), m= mass of active material (loading), and υ = scanning rate ($5mVs^{-1}$)

Sample	Surface Area per mass	Mass loaded/g	Overall surface area/ m^2	Specific capacitance/Fg^{-1}
0.01 KMnO4	74.6	0.00286	0.2134	95.76715
0.05 KMnO4	52.4	0.00223	0.1664	75.95944
Alpha-K	16.1	0.00240	0.0514	43.52651
Alpha K-free	19.0	0.00197	0.0211	23.98568

Figure 3: Table showing the results of the characterization of the samples

Figure 3 shows the results that we have gathered after the characterization of all samples. The area of CV graph of 0.01 M $KMnO_4$ sample is the greatest, followed by 0.05 M $KMnO_4$

sample, Alpha-K sample and Alpha K-free sample. Applying the area of CV graph to the equation above, we found that the specific capacitance of the 0.01 M $KMnO_4$ sample is the highest, followed by by 0.05 M $KMnO_4$ sample, Alpha-K sample and Alpha K-free sample.

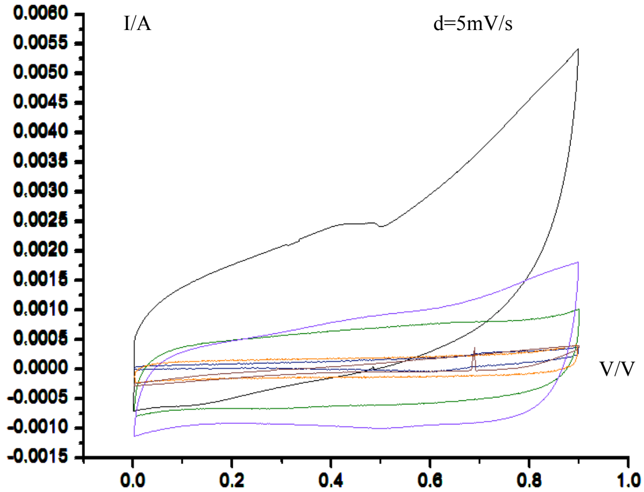

The specific surface area of each sample is calculated using BET. The 0.01 M $KMnO_4$ sample has surface/mass of 74.6 m^2g^{-1}, 0.05 M $KMnO_4$ sample 52.4 m^2g^{-1} , Alpha-K sample has 16.1 m^2g^{-1} and Alpha K-free sample has 19.0 m^2g^{-1}.

Specific surface area vs specific capacitance

The calculated specific capacitance is lower than normal possibly due to the difference in synthesis method as ours may be simplified. The increase in concentration had caused the nanoparticles to become bulky, while the increase in temperature had caused the nanoparticles to aggregate, reducing the surface area. This would cause the active sites of the nanoparticles to decrease, which would affect the capacitance of the sample as there will be less area for the deposition of the charges (in EDL supercapacitor).

This proves our hypothesis that the specific area of MnO_2 nanoparticles has a positive correlation to the specific capacitance of the material. On top of that, the ideal synthesis condition of MnO_2 to maximize the specific surface area would be to minimize the concentration of the precursor and decrease the temperature of the synthesis as much as possible.

Stabilising cation vs specific capacitance

It should be noted that despite the Alpha-K sample having greater specific capacitance, it has lower specific surface area than Alpha K-free sample.

This could be due to K^+ having a smaller radius as compared to H_3O^+ (Figure 5). This causes less steric hindrance hence allowing more efficient ion diffusion. This also shows that the size of the (2x2) tunnel is a determining factor in the specific capacitance of α -MnO_2. K^+ in aqueous solution has smaller radius than H_3O^+

Similarly, the specific surface area of the material is not the sole determinant of the specific capacitance of the material. Based on the result, the stabilizing cation seems to have a more significant impact in the specific capacitance as compared to the specific surface area.

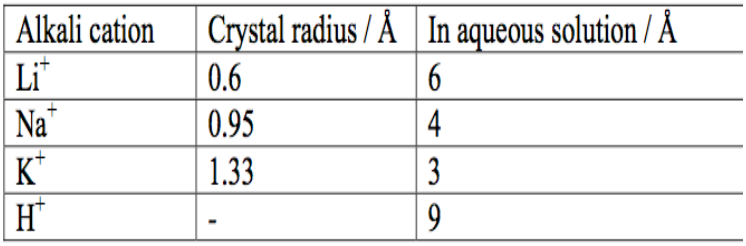

Alkali cation	Crystal radius / Å	In aqueous solution / Å
Li^+	0.6	6
Na^+	0.95	4
K^+	1.33	3
H^+	-	9

Figure 5: Table showing the different sizes of stabilising cations

CONCLUSION

We have found that there is a positive correlation between the specific surface area and the specific capacitance of the samples. The greater the specific surface area of the sample, the greater its ability to store charges will be. To maximize the specific surface area, the temperature of synthesis has to be minimized as well as the concentration of the precursor used.

However, specific surface area is not the sole determinant to the specific capacitance of the material. Changing the stabilizing cation from a larger cation to a smaller one will impact the specific capacitance in terms of the stability of the tunnel of the crystal structure as different cation has different positioning in the tunnel. In our case, The size of the tunnel positively correlate to the specific capacitance of the material. α -MnO_2 stabilised by K^+, a smaller cation, has greater specific capacitance than when it is stabilized by H_3O^+.

However this high capacitance is not maintained at high voltage. The stabilizing cation seems to have a greater impact in ensuring that the specific capacitance remains high at high voltage, as the sample with H_3O^+ has the highest rate capability.

For future work, we recommend investigating the optimum lowest temperature and concentration of precursor of the synthesis of α -MnO_2 in maximizing the specific surface area.

We also recommend growing the sample on the substrate itself, as this will create better contact, and lessen the charge transfer distance which could lessen the charge lost at high voltage. This will possibly lead to a higher rate capability of the sample. It is important to maintain high rate capability as it allows the supercapacitor to be versatile across voltages, allowing it to be used in various electronics.

We also have yet to explore other morphology (nanosheet, nanorods) as a method to increase specific capacitance. We are only using nanoflakes for this experiment. Certain morphology, like nanosheet, will have greater specific surface area, which will increase the specific capacitance. It remains to be tested whether the result of our experiment holds for all morphologies.

We believe that in the future, supercapacitors will be the main source of energy storage due to its high efficiency, especially in the face of energy scarcity, when supercapacitor is able to overcome its limitation in energy storage.

ACKNOWLEDGMENT

We would like to thank Wei Chao from Nanyang Technological University School of Material Science and Engineering for guiding us through the experiment and helping us with the necessary equipment used in the experiment. We would also like to thank Jeffrey Toh Ping Yong and Vincent Goh Wing Hoe of Anderson Junior College for mentoring us through the process.

REFERENCES

[1] Fan, Zhuangjun, Jun Yan, Tong Wei, Linjie Zhi, Guoqing Ning, Tianyou Li, and Fei Wei. 2011. 'Asymmetric Supercapacitors Based On Graphene/Mno2 And Activated Carbon Nanofiber Electrodes With High Power And Energy Density'. *Advanced Functional Materials* 21 (12): 2366-2375. doi:10.1002/adfm.201100058.

[2] Huang, Yi, Jiajie Liang, and Yongsheng Chen. 2012. 'An Overview Of The Applications Of Graphene-Based Materials In Supercapacitors'. *Small* 8 (12): 1805-1834. doi:10.1002/smll.201102635.

[3] Winter, Martin, and Ralph J. Brodd. 2004. 'What Are Batteries, Fuel Cells, And Supercapacitors?'.Cheminform 35 (50): 4245, 4266-4267.doi:10.1002/chin.200450265.

[4] Xu, Chengjun, Shan Shi, Yige Sun, Yanyi Chen, and Feiyu Kang. 2013. 'Ultrathin Amorphous Manganese Dioxide Nanosheets Synthesized With Controllable Width'. *Chem. Commun.* 49 (66): 7331. doi:10.1039/c3cc43055c.

[5] Zhi, Mingjia, Chengcheng Xiang, Jiangtian Li, Ming Li, and Nianqiang Wu. 2012. 'Nanostructured Carbon–Metal Oxide Composite Electrodes For Supercapacitors: A Review'. *Nanoscale* 5 (1): 72. doi:10.1039/c2nr32040a.

[6] Young, Matthias J., Aaron M. Holder, Steven M. George, and Charles B. Musgrave. 2014. 'Charge Storage In Cation Incorporated A-Mno2'. Chem. Mater., 141209160954008. doi:10.1021/cm503544e.

[7] Mao-wen Xu and Shu-Juan Bao (2011). Nanostructured MnO2 for Electrochemical Capacitor, Energy Storage in the Emerging Era of Smart Grids, Prof. Rosario Carbone (Ed.), ISBN: 978-953-307-269-2, InTech, Available from: http://www.intechopen.com/books/energy-storage-in-the-emerging-era-of-smart- grids/nanostructured- mno2-for-electro

[8] “High capacitance of electrodeposited MnO2 by the effect of a surface-active agent” **S. Devaraj** and N. Munichandraiah, **Electrochem. Solid-state Lett.,** 8, (2005) A 373.

[9] “Electrochemical supercapacitor studies of nanostructured α-MnO2 synthesized by microemulsion method and the effect of annealing” **S. Devaraj** and N. Munichandraiah, **J. Electrochem. Soc.,** 154 (2007) A80.

[10] “Effect of crystallographic structure of MnO2 on its electrochemical capacitance properties” **S. Devaraj** and N. Munichandriah, **J. Phys. Chem. C** 112 (2008) 4406.